Environmental
Science
Processes & Impacts

Emerging Investigator Series: Sunlight Photolysis of 2,4-D Herbicides in Systems Simulating Leaf Surfaces

SCHOLARONE™
Manuscripts

1
2
3   1
4
5   2
6
7   3
8
9   4
10
11   5
12
13   6
14
15   7
16
17   8
18
19   9
20
21   10
22

Emerging Investigator Series: Sunlight Photolysis of 2,4-D Herbicides in Systems Simulating Leaf Surfaces

Lei Su[1], John D. Sivey[2], Ning Dai[1*]

[1]Department of Civil, Structural and Environmental Engineering

University at Buffalo, The State University of New York

Buffalo, New York 14260, United States

[2]Department of Chemistry

Towson University

Towson, Maryland 21252, United States

*Corresponding author: Post address: 231 Jarvis Hall, Buffalo, NY 14260

Phone: (716) 645-4015; Fax: (716) 645-3667

Email: ningdai@buffalo.edu

32   **ABSTRACT**

33   Pesticides are commonly applied on foliage, forming dry deposits on the leaf cuticular

34   wax. However, their photochemical transformation in this lipophilic environment is much less

35   understood compared with that in surface water. In this work, sunlight photolysis of six

36   chlorinated phenoxyacetic acid herbicides (i.e., 2,4-D and structural analogues) was evaluated in

37   four organic solvents, on quartz, and on paraffin wax. In solvents of low polarity (i.e., *n*-heptane

38   and 2-propanol), direct photolysis of 2,4-D herbicides was enhanced due to the relatively high

39   quantum yields in these solvents. Photolysis on paraffin wax was slower than photolysis on

40   quartz by a factor of 3–9, but was comparable with that in solvents of low polarity. With

41   environmentally relevant irradiation and surface loading, the half-lives of 2,4-D herbicides on

42   paraffin wax were 27–159 h, which are within the same range reported for biodegradation, the

43   dominant dissipation pathway in the current 2,4-D fate model. Product analyses showed that

44   photoreductive dechlorination is the dominant pathway in organic solvents, accounting for 68–

45   100% of parent compound decay. On quartz and paraffin wax surfaces, however, photoreductive

46   dechlorination products accounted for < 60% of parent compound decay. Combining kinetic

47   modeling and product analyses, it was shown that neither could the two additional putative

48   pathways (photosubstitution of chlorine by hydroxyl group and cleavage of the ether bond) fully

49   account for the total phototransformation on surfaces. These results suggest that rapid photolysis

50   on surfaces can be attributed to unique pathways that are absent in the organic solvent phase.

51   **Environmental significance**

52   Pesticides are often applied on foliage, but their photolysis in this environment is much

53   less understood compared with that in water. This study systematically investigated the

54   photolysis of 2,4-D herbicides in systems simulating the reaction environment of leaf surface,

55   including non-polar organic solvents and quartz and wax surfaces. We determined photolysis

56   rate constants and quantum yields, and analyzed photoproducts. Our results showed that direct

57   photolysis of 2,4-D herbicides on paraffin wax can be as fast as their biodegradation in water, the

58   dominant degradation pathway considered in the current fate model. Additionally, the major

59   reaction pathway in organic solvents and on surfaces (i.e., photoreductive dechlorination) is

60   distinct from that previously reported in water.

1   Introduction

61

62   Photochemical transformation is a major pathway for pesticide degradation.[1] In a recent

63   review, more than half of the 160 pesticides evaluated undergo direct photolysis under sunlight,

64   with half-lives as short as 2 h.[2] For pesticides that do not absorb sunlight, indirect photolysis

65   (i.e., photolysis sensitized by natural organic matter, nitrate, or iron species) can be an important

66   dissipation pathway.[3-5]

67   Pesticides that are applied directly on foliage form dry deposits on the cuticular wax of

68   leaves.[6] Nevertheless, their photochemical transformation on leaves is much less understood

69   compared with that in surface water. Lipophilic environments, such as cuticular wax,[7] have been

70   shown to promote direct photolysis by extending the life-times of excited state molecules.[8]

71   Spruce needle wax was shown to serve as a hydrogen donor in the photoreductive dechlorination

72   of some persistent organic pollutants (e.g., benzophenone and DDT).[9] Additionally, when

73   present as dry deposits, pesticide molecules may exhibit light absorption properties different

74   from those in the solvent phase,[1] and may favor reaction pathways that minimize conformation

75   change between reaction intermediates and parent compounds.[10]

76   Previous studies[11-15] of the photochemical transformation of pesticides on leaves used

77   two types of model systems. In the first type, organic solvents were used to represent specific

78   components of the cuticular wax. For example, cyclohexane and cyclohexene were used as

79   surrogates of the saturated and unsaturated hydrocarbons, respectively, of cuticular wax.[11, 12] The

80   direct photolysis of fungicide folpet and insecticide parathion was 10–100 times faster in

81   cyclohexene than in cyclohexane, suggesting that their photolysis proceeds more efficiently in

82   olefinic media.[11, 12] When DDT, methoxychlor, and anilazine were irradiated in methyl oleate, a

83   surrogate of the octadecenoic acids in cuticle wax, photoinduced addition of pesticides to methyl

84   oleate was observed, suggesting that the solvent molecules directly participated in pesticide

85   phototransformation.[13, 14] In methanol and 2-propanol representing the primary and secondary

86   alcohol groups, respectively, common in cuticular wax, cyclohexanedione oxime herbicides

87   clethodim and sethoxydim photodegraded 3–5 times faster than in water.[15] The potential

88   influence of solvent polarity on pesticide photolysis, however, was not considered in these

89   studies.[11-15]

90   The second type of model system employs surfaces with different physicochemical

91   characteristics, such as glass,[16-19] silica gel,[20, 21] or a thin layer of wax extracted from leaves.[20, 22-

92   26] Differences between direct photolysis rates on surfaces compared to those in solutions vary

93   among pesticides. Fungicide hexachlorobenzene persisted on glass surface after 5 months of

94   irradiation by artificial sunlight, but achieved 70% decay in methanol after 15 days under

95   sunlight.[27] In contrast, fungicide guazatine-triacetate degraded 67% after 84 h when present as a

96   thin film on glass surface, but no degradation was observed in water or methanol.[18] More

97   recently, Richard and co-workers[26] developed a procedure to create simulated leaf surfaces by

98   extracting wax from plants and reconstituting it on dishes. On the extracted maize and carnauba

99   gray wax, photolysis rates of triketone herbicides were 10–900 times faster than those in water.[26,

100   28]

101   Although differences in the photochemical behavior of pesticides in water and on

102   surfaces have been documented, mechanistic interpretations have been scarce due to insufficient

103   experimental controls in many of the studies employing surfaces. For example, surfactants are a

104   common adjuvant in commercial pesticide formulations; however, some previous studies

105   employed pure pesticides,[15, 29] which could form aggregates capable of interfering with light

106   absorption. Surfactants have only recently been considered as an important adjuvant in

107   photolysis experiments.[30] Additionally, most of the reported irradiation intensity was based on

108   the output of the light sources,[19, 20, 23-25] which cannot account for the variation in light

109   attenuation attributable to differences in reactor geometry between solvent and surface

110   experiments.

111   The goal of this work is to investigate the direct photolysis of 2,4-dichlorophenoxyacetic

112   acid (2,4-D) and five related herbicides (Table 1) under conditions relevant to leaf surfaces. 2,4-

113   D is an herbicide (frequently formulated as an ester) that is widely applied post-emergence to

114   control broadleaf weeds. Developed in the 1940s, 2,4-D remains the 7th most used agricultural

115   pesticide and the most used pesticide in non-agricultural sectors.[31] In surface water, sunlight

116   photolysis of 2,4-D and related herbicides is slow. For example, the photolysis half-life of 2,4-D

117   in water is 13 d,[32] while its biodegradation half-life is 30 to 40 h.[33] On leaf surfaces, however,

118   photolysis may play a more significant role due to the lower microbial activity and the potential

119   enhancement of photolysis by leaf surfaces.

120   In this work, direct photolysis of six chlorinated phenoxyacetic acid herbicides was

121   examined in organic solvents and on surfaces under simulated sunlight. First, photolysis rate

122   constants, molar extinction coefficients, and quantum yields were determined in four organic

123   solvents with different polarity and hydrogen-donating ability. Subsequently, photolysis

124   experiments were conducted on quartz and paraffin wax surfaces, and the reaction rate constants

125   were compared with those obtained from solvent experiments. For selected herbicides,

126   photodegradation products in organic solvents and on surfaces were analyzed. Lastly, the

127   photolysis mechanisms relevant to leaf surfaces were discussed.

128   **2   Materials and Methods**

129   **2.1   Materials**

130　　　Detail information on the chemicals used in this study is shown in Text S1.

131　**2.2　Photolysis Experiments**

132　　　A total of six structurally related phenoxyacetic acid herbicides were used (Table 1).

133　Among them, 2,4-D and 2,4-DBEE are widely used in commercial formulations, while 2,4-DME

134　and 2,4,5-T and its esters are banned in the United States due to their high volatility and/or high

135　toxicity,[34] but are still used in other parts of the world.[35] For photolysis experiments in the

136　solvent phase, pesticide stock solutions were prepared from pure compounds or used as

137　purchased. The solvent of the stock solutions was selected based on pesticide solubility limits.

138　Accordingly, some reaction solutions contained more than one solvent (Table S1), but the co-

139　solvent was less than 1.5 vol% in all reaction solutions except for 2,4-D and 2,4,5-T. The initial

140　concentrations of 2,4-D and 2,4,5-T in the reaction solutions were 20 µM and those of 2,4-DME,

141　2,4,5-TME, 2,4-DBEE, and 2,4,5-TBEE were 5 µM. Aqueous reaction solutions were buffered

142　with phosphate (pH 7.0, 5 mM).

143　　　For surface experiments, quartz dishes (diameter: 55 mm, depth: 15 mm, capacity: 20

144　mL) were used to provide quartz surfaces. To prepare paraffin wax surfaces, glass petri dishes

145　were dipped in melted paraffin wax (110 °C for 20 minutes), and then placed horizontally and

146　cooled at room temperature to form a flat surface. The wax surfaces were inspected visually. No

147　solvent pooling was observed during sample loading (see below). The wax coated dishes have

148　the same dimensions as the quartz dishes. To apply pesticides on the surfaces, a mixture of the

149　surfactant Tween® 20 and the target pesticide, dissolved in methanol or acetonitrile (3 mL), was

150　added to the dishes. Because paraffin wax surface is more hydrophobic than quartz, a higher

151　concentration of Tween® 20 was used on wax (10:1 molar ratio to the pesticide) than on quartz

152　(1:1 molar ratio). The dishes were stored in the dark for 3–12 h to allow solvent to evaporate.

153   Experimental verification (e.g., via microscopy) of surface dryness following the solvent

154   evaporation time was not performed. The recoveries of pesticides from the two surfaces were in

155   the range of 87.8%–99.8% (Table S2), suggesting there was no substantial loss during sample

156   loading or analysis (described below in section 2.3). The pesticide surface loading used in the

157   experiments (3×10^{-9} mol cm^{-2}) was similar in magnitude as the 2,4-D application rate in the

158   field (265 g per hectare, equivalent to 1.2×10^{-8} mol cm^{-2}).[36] During preparation of surface

159   samples, a sodium lamp (λ = 589 nm) was used for laboratory illumination to minimize

160   photolysis loss.

161   Photolysis experiments were conducted in a Q-SUN Xe-1 test chamber equipped with a

162   Xenon arc lamp to produce the full sunlight spectrum. A daylight-Q filter (X-7460) was used to

163   remove irradiation below 290 nm to simulate direct sunlight at the Earth's surface. The lamp was

164   set to a light intensity of 0.68 W m^{-2} at 340 nm, and the total irradiation intensity was determined

165   using chemical actinometry (see section 2.4 below). A circulating water bath was used to

166   maintain sample temperature at 26 ± 3 ºC. For liquid samples, each reaction solution (10 mL)

167   was placed in a quartz test tube capped with a silicone stopper. The test tubes were placed in the

168   water tank at a 45° angle. At selected time points, 0.5 mL of reaction solution was removed from

169   each test tube for analysis. For surface samples, dishes loaded with pesticides were covered by

170   quartz disks and placed in the sunlight test chamber (half submerged in the circulating water

171   bath). Dishes were removed at selected time points for analysis. All experiments were conducted

172   in duplicates and included dark control samples.

173   **2.3   Sample Analysis**

174   For solvent experiments, the 2,4-D and 2,4,5-T samples were analyzed using high

175   performance liquid chromatography with a diode array detector (HPLC-DAD, Agilent 1260

176 Infinity), and the methyl and butoxyethyl ester samples from solvent experiments were analyzed

177 by gas chromatography-mass spectrometry (Agilent Model 7890B GC-240 MS) with chemical

178 ionization using methanol. For surface experiments, the residual pesticides were dissolved by

179 methanol and analyzed by HPLC-DAD. The details of the analytical methods are shown in Text

180 S2.

181   Photoproducts for the trichlorinated phenoxyacetic acid herbicides were evaluated.

182 HPLC-DAD was first used to quantify the dechlorination products of 2,4,5-T, 2,4,5-TME, and

183 2,4,5-TBEE (i.e., 2,4-D, 2,4-DME, 2,4-DBEE, and their isomers), as well as 2,4,5-

184 trichlorophenol, the potential product from the cleavage of the ether bond. Because the isomers

185 of 2,4-D and 2,4-DBEE were not commercially available, the total concentrations of isomers

186 were estimated using the HPLC calibration curve for 2,4-D and 2,4-DBEE, respectively. Further

187 discussion on this methodology is provided in section 3.3. The methanol and 2-propanol solvent

188 samples and the methanol extracted surface samples were directly analyzed. For the *n*-heptane

189 samples of 2,4,5-TBEE, 1 mL of sample was blown down by nitrogen gas to dryness in an amber

190 vial, and reconstituted in 1 mL methanol and immediately analyzed by HPLC-DAD. The

191 recovery of 2,4-DBEE using this method was 102.8% ± 1.3%. Methyl esters were too volatile to

192 be recovered using solvent blowdown; therefore, the *n*-heptane samples of 2,4,5-TME photolysis

193 were not analyzed for photoproducts. The HPLC method for product analysis is described in

194 Text S2.

195   GC-MS (full scan) was used to explore other products for 2,4,5-TME photolysis in the

196 solvents. Authentic 2,4-DME standard was used to verify one of the product peaks from 2,4,5-

197 TME photolysis in solvents. The GC-MS method for product analysis is described in Text S2.

198   The 2,4,5-T and 2,4,5-TBEE surface samples were also analyzed using ultra-performance

199   liquid chromatography interfaced with high-resolution, quadrupole/time-of-flight mass

200   spectrometer using an electrospray ionization source (operated in negative ionization mode)

201   (UPLC-ESI(-)-qTOF). Methanol was used to extract the photoproducts from the surfaces and

202   blown down to dryness under nitrogen gas. The samples were reconstituted in acetonitrile for

203   UPLC-ESI(-)-qTOF analysis. Product identification was based on accurate mass measurement.

204   The details of the UPLC-ESI(-)-qTOF method are shown in Text S2.

205   **2.4   Determination of Quantum Yield**

206   Equation 1 describes the kinetics of a photolysis reaction.[37]

$$-\frac{dC}{dt} = \sum \Phi_\lambda \left[\frac{E_p^0(\lambda)}{d} \right] \left[1 - 10^{-(\alpha_\lambda + \varepsilon_\lambda C)d} \right] \left[\frac{\varepsilon_\lambda C}{\alpha_\lambda + \varepsilon_\lambda C} \right]$$

207   Eq. 1

208   where C is the pesticide concentration (mol L^{-1}) at time t (s); Φ_λ is the quantum yield of pesticide

209   decay (dimensionless) at wavelength λ; $E_p^0(\lambda)$ is the incident light intensity (Einstein cm^{-2} s^{-1}) at

210   wavelength λ; d is the sample pathlength (cm); α_λ is the absorption coefficient of the reaction

211   matrix (cm^{-1}); ε_λ is the molar extinction coefficient of the pesticide (L mol^{-1} cm^{-1}).

212   Equation 1 can be simplified to pseudo first-order kinetics (equation 2) if the following

213   two constraints are met: (1) light absorption by the reaction matrix is not significant (i.e., $\varepsilon_\lambda C \gg$

214   α_λ), and (2) total light absorption by pesticide and reaction matrix together is small, $F_{s\lambda} < 0.1$,

215   where $F_{s\lambda}$ is the fraction of light absorbed by the system as determined from the absorption

216   spectrum (equation 3).[37]

$$-\frac{dC}{dt} = 2.303 \sum \Phi_\lambda E_p^0(\lambda)\varepsilon_\lambda C = -kC$$

217   Eq. 2

$$F_{s\lambda} = 1 - 10^{-(\alpha_\lambda + \varepsilon_\lambda C)d}$$

218   Eq. 3

9

219   In our experiments (sunlight spectrum), both criteria are satisfied: the solvents have

220   negligible absorbance and the reaction solutions exhibited low optical density. For example, the

221   maximum $F_{s\lambda}$ for 2,4-D in phosphate-buffered water is 0.09 at the absorption maximum 290 nm.

222   Quantum yield Φ_{λ} was assumed to be wavelength independent within the sunlight spectrum.[37]

223   Accordingly, quantum yield can be calculated as equation 4.

$$\Phi = \frac{k}{2.303\sum E_p^0(\lambda)\varepsilon_{\lambda}}$$

224   Eq. 4

225   where k is the pseudo first-order rate constant of pesticide photolysis reaction (s^{-1}).

226   The molar extinction coefficients ε_{λ} for pesticides in solvents were calculated using the

227   Beer-Lambert Law based on the absorption spectra (200–800 nm) measured by an Agilent Cary

228   60 UV-Vis spectrophotometer. The background absorption of the respective solvent was

229   subtracted. The molar extinction coefficients of pesticides on quartz were also estimated: a

230   quartz dish loaded with a pesticide compound (6.17×10^{-8} mol cm^{-2}; Tween® 20 to pesticide

231   molar ratio 5:1) was placed in the spectrophotometer, and the light transmission was compared

232   with that measured through a disk loaded with surfactant alone. The difference was used to

233   approximate the absorbance of pesticides in the solid form. Further details on the measurement

234   of absorbance on quartz surface are provided in Text S4. The molar extinction coefficients of

235   pesticides on wax cannot be determined using this method due to the negligible light

236   transmission through wax. Additionally, because light scattering by pesticides and reflection by

237   the quartz surface is not accounted for, this measurement yields the upper bound of molar

238   extinction coefficients for pesticides on quartz. The molar extinction of a pesticide in solid form

239   is calculated by equation 5.

$$\varepsilon_{\lambda} = \frac{A}{q} \times 10^{-3} (\text{L cm}^{-3})$$

240   Eq. 5

10

241 where A is the absorbance (dimensionless) measured by UV-Vis spectrophotometry, and q is the

242 surface concentration (mol cm^{-2}).

243   Chemical actinometry was used to determine the quantum yields of pesticides in different

244 reaction environments. 2-Nitrobenzaldehyde (2-NB) was used as the actinometer, and its decay

245 was monitored. The photolysis of 2-NB occurs intramolecularly with a reported quantum yield of

246 0.41.[38, 39] Studies have shown that the quantum yield of 2-NB is independent of temperature,

247 solvent, and the state of the molecule (e.g., dissolved or solid).[38-42] 2-NB can be used either at a

248 high concentration (e.g., 0.1 M), where it absorbs all incident light and exhibits pseudo zero-

249 order photolysis kinetics or at a low concentration (e.g., 10 µM), where it exhibits pseudo first-

250 order photolysis kinetics.[38, 42] For the solvent phase experiments, a low concentration (10 µM) of

251 2-NB aqueous solution was used, for which equation 2 applies for its pseudo first-order kinetic

252 decay. Thus, the quantum yield for each pesticide can be calculated using equation 6. For the

253 solvent experiments, the simulated sunlight intensity was 320 W m^{-2} as determined by the

254 actinometer 2-NB.

$$\Phi_{pesticide} = \Phi_{2-NB} \times \frac{k_{pesticide}}{k_{2-NB}} \times \frac{\sum E_p^0(\lambda)_{2-NB}\, \varepsilon_{\lambda,2-NB}}{\sum E_p^0(\lambda)_{pesticide}\, \varepsilon_{\lambda,pesticide}}$$

255   Eq. 6

256   To quantify light intensity on surfaces, 2-NB was applied on dish surface in the same

257 fashion and at the same loading as the pesticides (3×10^{-9} mol cm^{-2}). The molar ratios of

258 Tween$^{®}$ 20 to 2-NB was 1:1 and 10:1 for experiments on quartz and paraffin wax, respectively.

259 Photolysis of 2-NB was performed under the same irradiation condition as pesticide surface

260 samples. After irradiation, 3 mL and 5 mL of deionized water, respectively, were added to the

261 dishes with quartz or paraffin wax surfaces to dissolve residual 2-NB, and samples were taken

262 after 5 min for analysis. The recovery of 2-NB on surfaces was between 92.8% and 95.7%

263   (Table S2). 2-NB was analyzed with HPLC-DAD. 2-NB eluted at 1.52 min with 60% Milli-Q

264   water and 40% acetonitrile (flow rate 1 mL min^{-1}) and was detected at 230 nm. The molar

265   extinction coefficient of the actinometer 2-NB on quartz surface was measured in the same way

266   as that for the pesticides.

267   **3.   Results and Discussion**

268   **3.1   Photolysis of Chlorinated Phenoxyacetic Acid Herbicides in Solvents**

269   Direct photolysis of the six chlorinated phenoxyacetic acid herbicides was first

270   investigated in solvents spanning a range of polarities: water, acetonitrile, methanol, 2-propanol,

271   and *n*-heptane. Due to solubility constraints, 2,4-D and 2,4,5-T were not evaluated in *n*-heptane.

272   Preliminary experiments showed that the ester compounds hydrolyzed rapidly in water: less than

273   10% of the initial 2,4-DME and 2,4,5-TME mass remained in water after 6 h in the dark, which

274   is consistent with previous reports of facile hydrolysis of these esters.[43] Therefore, the photolysis

275   of the four ester compounds was not evaluated in water. Additionally, we observed that

276   significant transesterification occurred between butoxyethyl esters and methanol in the dark; less

277   than 30% of the initial 2,4,5-TBEE mass remained in methanol after 48 h in the dark (Text S3).

278   Thus, photolysis experiments of butoxyethyl esters were not performed in methanol.

279   Upon irradiation, all six compounds decayed following apparent first-order kinetics

280   (Figure S1A–F). No degradation was observed in dark control samples (data not shown). The

281   apparent first-order photolysis rate constants in different solvents are shown in Figure 1 (left

282   panel) and Table S3. Among the organic solvents tested, 2-propanol featured the fastest 2,4-D

283   and 2,4,5-T photolysis. Methanol and acetonitrile yielded similar rate constants, 6–11 times

284   lower than 2-propanol. For the four ester derivatives (2,4-DME, 2,4,5-TME, 2,4-DBEE, and

285   2,4,5-TBEE), a similar trend was observed: photolysis was fastest in *n*-heptane, followed by 2-

286   propanol, methanol, and acetonitrile. The photolysis rate constants for 2,4-DME, 2,4,5-TME,

287   2,4-DBEE, and 2,4,5-TBEE in *n*-heptane were 2–4 times higher than the corresponding rate

288   constants in 2-propanol. Photolysis of methyl esters in 2-propanol was 6–9 times faster than that

289   in methanol and at least 35 times faster than that in acetonitrile. In the same solvent, the rate

290   constants across different phenoxyacetic acid herbicides were within the same order of

291   magnitude.

292   Given that the polarity of the solvents followed the order *n*-heptane < 2-propanol <

293   methanol ≈ acetonitrile, the results suggested that faster photolysis occurred in solvents of lower

294   polarity. The correlation between photolysis rate constants and solvent polarity (measured by the

295   dielectric constant) is shown in Figure S3. The influence of organic solvent polarity on the direct

296   photolysis of chlorinated phenoxyacetic acid herbicides is consistent with that observed for the

297   persistent organic pollutant octachlorodibenzo-*p*-dioxin and azoxystrobin fungicide, which

298   photodegraded faster in organic solvents of lower polarity.[8, 44, 45] However, the opposite trend

299   was reported for polycyclic aromatic hydrocarbons and the vitamin riboflavin, both of which

300   photodegraded faster in solvents of higher polarity (e.g. water, acetonitrile, and methanol) than in

301   solvents of lower polarity (e.g. ethyl acetate, cyclohexane, and hexane).[46-48] It is worth noting

302   that the trend observed for organic solvents does not extend to water, the most polar solvent

303   tested in this study. For example, 2,4,5-T photolysis in water (pH 7.0) was three times faster than

304   that in methanol and acetonitrile, although still 3 times slower than in 2-propanol. This may be

305   attributed to the different reaction pathways dominating in water compared to those occurring in

306   organic solvents (see further discussion in section 3.5).

307   To differentiate whether solvents influenced photolysis by altering light absorption of

308   herbicides or by altering their reaction pathways, the molar extinction coefficients in different

309   solvents were determined (Figure 2 and S2). As solvent polarity increases in the order of *n*-

310   heptane < 2-propanol < methanol ≈ acetonitrile, the absorption spectra of all chlorinated

311   phenoxyacetic acid herbicides exhibited a slight blue shift, but the shift was less than 1 nm at the

312   absorption peaks near 290 nm. Considering the absorption spectra of the chlorinated

313   phenoxyacetic acid herbicides and the sunlight spectrum, the amount of light absorbed can be

314   calculated by $\int E_p^0(\lambda)\varepsilon_\lambda d\lambda$, integrated across wavelength 290–315 nm (Table S4). The

315   variation of light absorption by pesticides in different solvents was within 41%, substantially

316   smaller than the variation of their photolysis rate constants.

317   The quantum yields for the six chlorinated phenoxyacetic acid herbicides were calculated

318   using equation 6 and are shown in Figure 3 and Table S3. The relative magnitude of quantum

319   yields in different organic solvents was similar to that of the apparent first-order rate constants

320   (*n*-heptane > 2-propanol > methanol ≈ acetonitrile), as would be expected from the small

321   difference in light absorption in different solvents. The quantum yields of 2,4-DME and 2,4-

322   DBEE in *n*-heptane were 2.4×10^{-2} and 1.7×10^{-2}, respectively, which is lower than those

323   previously reported in *n*-hexane and *n*-hexadecane (0.13–0.17).[43] The reason for this discrepancy

324   is unknown.

325   **3.2**   **Photolysis of Chlorinated Phenoxyacetic Acid Herbicides on Quartz and Paraffin**

326   **Wax Surfaces**

327   The direct photolysis of 2,4-D, 2,4,5-T, 2,4-DBEE, and 2,4,5-TBEE was examined on

328   quartz and paraffin wax surfaces. The two methyl esters were not evaluated due to their high

329   volatility. Similar to that in the bulk solvent phase, photolysis on surfaces also followed apparent

330   first-order kinetics (Figure S1G and S1H). No degradation was observed in dark control samples

331   (data not shown).

14

332   The apparent first-order rate constants for pesticide photolysis on surfaces are shown in

333   Figure 1 (right panel) and Table S3. For all four compounds, photolysis was 3–9 times faster on

334   quartz than on paraffin wax. Lower surfactant loading was used on quartz surface due to its

335   lower hydrophobicity than wax. Nevertheless, differences in surfactant loading are unlikely to

336   account for the faster photolysis on quartz based on two lines of evidence: first, Tween[®] 20 has

337   negligible sunlight absorption (Figure S4); second, the photolysis rate constants were not

338   significantly different between experiments in which the molar ratios of 2,4,5-TBEE to Tween[®]

339   20 was 1:1 (0.22 ± 0.0088 h^{-1}) compared to 1:10 (0.22 ± 0.0077 h^{-1}). Neither can the difference

340   be attributed to higher effective light intensity on quartz, because the chemical actinometer 2-

341   NB, which photodegrades via intramolecular rearrangement, decayed at similar rates on quartz

342   and on wax surfaces (< 12% difference, Figure S1I). Previously, herbicide isoproturon and plant

343   activator acibenzolar-*S*-methyl were also reported to photodegrade faster on glass than on

344   paraffin wax and leaf-extracted cutin surface by a factor of 1–3 upon UV and sunlight

345   irradiation.[49, 50]

346   When compared with photolysis in solvents, photolysis on quartz was much faster. The

347   rate constants of 2,4-D and 2,4,5-T photolysis on quartz were 34 and 8 times higher,

348   respectively, than the corresponding rate constants in 2-propanol, where their photolysis was the

349   fastest among the solvents tested. 2,4-DBEE and 2,4,5-TBEE photolysis on quartz were 2 and 3

350   times faster than in *n*-heptane. In comparison, photolysis on paraffin wax proceeded at similar

351   rates as that in solvents of low polarity (i.e., *n*-heptane and 2-propanol). The difference in

352   photolysis rates among the four compounds on the same surface was within a factor 7.

353   The observation that chlorinated phenoxyacetic acid herbicides photodegraded faster on

354   quartz surface than in organic solvents (i.e., 2-propanol, methanol and acetonitrile) and water is

15

355　opposite to the trends observed for herbicides clethodim and sethoxydim[15] and fungicide

356　benzothiostrobin,[29] but is consistent with those for fungicide guazatine, and herbicides bentazon,

357　clopyralid, sulcotrione, and mesotrione.[6, 18, 26, 28] In the first two studies,[15, 29] pesticide solutions

358　were directly pipetted onto the glass surface without surfactant, while the other studies[6, 18, 26, 28]

359　used surfactants to load pesticides or used commercial formula that contained surfactants.

360　Therefore, the slow photolysis on surface observed in the first two studies was likely attributable

361　to the interference of light absorption by pesticide aggregates.

362　　　Out of the four organic solvents and two surface systems tested in this study, paraffin

363　wax surface best simulates the reaction environment on leaves. Using the photolysis rate

364　constants shown in Figure 1 (320 W m^{-2} sunlight intensity) and accounting for the diurnal change

365　in sunlight intensity for a midsummer day at 40° N" latitude (sea level) under clear skies,[3, 51] the

366　half-lives of 2,4-D, 2,4,5-T, 2,4-DBEE, and 2,4,5-TBEE were estimated to be 72, 42, 159, and

367　27 h, respectively. With the possible exception of 2,4-DBEE, these photolysis half-lives are on

368　the same order of magnitude as the half-lives previously reported for biodegradation (30–40 h),[33]

369　which is noteworthy given that biodegradation is currently considered as the major dissipation

370　pathway for these herbicides.[52]

371　　　As shown in Figure 2 and S2, the experimentally determined molar extinction

372　coefficients of chlorinated phenoxyacetic acid herbicides on quartz surface, despite being the

373　upper bound (section 2.4), is significantly lower than those in the solvent phase. The quantum

374　yields on quartz calculated using these molar extinction coefficients are therefore the lower

375　bound of the true values, but they are still greater than those in the solvent phase. For example,

376　the calculated quantum yields for 2,4-D and 2,4,5-T on quartz (0.12 and 0.070, respectively) are

377　38 and 6.4 times higher than those in 2-propanol, and the calculated quantum yields for 2,4-

378　DBEE and 2,4,5-TBEE on quartz (0.074 and 0.028, respectively) are 4.3 and 1.2 times higher

379　than those in *n*-heptane. Our results are among the very first attempts to quantify quantum yields

380　for pesticide photolysis on surfaces. The only other such report[53] was on the quantum yield of

381　imidacloprid, a neonicotinoid insecticide, on the top surface of a clean germanium ATR crystal

382　$(1.6 \times 10^{-3}$ at 305 nm), and showed that it was 3–9 times smaller than that in water. Because the

383　molar extinction coefficients on wax cannot be determined using the absorbance method (section

384　2.4), the corresponding quantum yields were not calculated.

385　**3.3　Photoproducts of Chlorinated Phenoxyacetic Acid Herbicides in Organic Solvents**

386　　　　Previous research suggested that 2,4-D and its esters undergo photolysis via three

387　pathways in water: (I) photoreductive dechlorination, (II) photosubstitution of chlorine by a

388　hydroxyl group, and (III) cleavage of the ether bond (Figure 4 showing 2,4,5-T and its esters).[43,]

389　[54, 55] Because photoreductive dechlorination was previously reported as a major pathway for the

390　photolysis of 2,4-DME and 2,4-DBEE in non-polar solvents hexane and hexadecane,[43] the

391　corresponding products were first targeted in the organic solvent samples of 2,4,5-TBEE and

392　2,4,5-TME.

393　　　　For 2,4,5-TBEE, samples in *n*-heptane and 2-propanol were analyzed but not those in

394　acetonitrile due to insignificant 2,4,5-TBEE decay (< 10% after 72 h). Photoreductive

395　dechlorination of 2,4,5-TBEE can form three isomeric butoxyethyl dichlorophenoxyacetates

396　(DBEEs, i.e., 2,4-DBEE, 2,5-DBEE, and 3,4-DBEE), but an authentic standard is only available

397　for 2,4-DBEE. Because of the similar octanol-water partition coefficients of the three isomers,[56-]

398　[58] it was hypothesized that they would have very similar retention times in HPLC. We observed

399　only one peak at the retention time corresponding to 2,4-DBEE, suggesting that either all three

400　isomers co-eluted or 2,4-DBEE was the dominant product. Additionally, it was estimated that the

401 three isomers would feature similar molar extinction coefficients at 230 nm (the DAD detection

402 wavelength) with difference within 5%, which was the difference between the molar extinction

403 coefficients for 2,4-DBEE and 2,4,5-TBEE in methanol at 230 nm (Table S5). Accordingly, the

404 total amount of DBEEs were estimated using the 2,4-DBEE calibration curve. Figure 5A shows

405 the evolution of DBEEs in *n*-heptane and 2-propanol from 2,4,5-TBEE photolysis. In the early

406 phase of the experiments (i.e., < 40% 2,4,5-TBEE decay), DBEE formation accounted for all of

407 the 2,4,5-TBEE decay. With more extensive 2,4,5-TBEE decay, the accumulation of DBEEs

408 deviated from the 1:1 line, which may be attributed to their further photolysis. Indeed, a new

409 HPLC peak, with a shorter retention time than the DBEE peak, appeared in the *n*-heptane sample

410 when > 83% of the initial 2,4,5-TBEE had decayed.

411 Using a similar method, the methyl dichlorophenoxyacetates (DMEs, i.e., 2,4-DME, 2,5-

412 DME, and 3,4-DME) were quantified in the 2,4,5-TME samples in 2-propanol and methanol

413 (Figure 5B). In both solvents, the formation of DMEs accounted for 68–100% of 2,4,5-TME

414 decay throughout the experiment. The *n*-heptane samples for 2,4,5-TME photolysis were not

415 analyzed by HPLC due to the extensive loss (presumably due to volatilization) during solvent

416 exchange for reverse-phase HPLC analysis. However, the formation of the three DMEs from

417 2,4,5-TME photolysis in *n*-heptane, as well as in 2-propanol and methanol, was confirmed by

418 GC-MS using chemical ionization and the full scan mode of MS. The most distinct product

419 peaks for the irradiated 2,4,5-TME samples are three consecutive peaks with retention times of

420 less than 0.2 min apart (Figure 6). These peaks show identical mass spectra featuring m/z 235,

421 237, and 239 with a ratio 9:6:1 (Figure S7B–D), which suggest the presence of two chlorine

422 atoms in the molecule. The second peak was confirmed as 2,4-DME (298.3 ± 25.0 °C)[57] using an

423 authentic standard. Based on the boiling points of the three isomers,[56, 58] it was suspected that the

424   first and third peaks were 2,5-DME (296.1 ± 25.0 °C), and 3,4-DME (302.9 ± 27.0 °C),

425   respectively. The signal intensity for all three isomers increased as 2,4,5-TME degraded (Figure

426   S6). For the 2-propanol and methanol samples (up to 24% 2,4,5-TME decayed), the GC-MS

427   spectra did not show other product peaks (cutoff signal to noise ratio of 5). For the *n*-heptane

428   sample in which 86% of 2,4,5-TME decayed, an additional product peak was detected with a

429   retention time shorter than 2,4-DME and a mass spectrum consistent with the presence of one

430   chlorine atom (m/z 201 and 203, ratio 3:1, Figure S7E). This suggests that the DMEs can further

431   degrade to form monochlorinated products. This observation also suggests that the unidentified

432   HPLC peak observed in the irradiated 2,4,5-TBEE *n*-heptane samples could be a butoxyethyl

433   chlorophenoxyacetate. 2,4,5-TBEE samples cannot be analyzed by GC-MS because of the low

434   thermal stability of butoxyethyl group, which can introduce GC artifacts.

435   The formation of 2,4,5-trichlorophenol, the product anticipated from the cleavage of the

436   ether bond of 2,4,5-TBEE and 2,4,5-T (pathway III),[43, 54, 59] was monitored using HPLC, but its

437   concentration was below the detection limit in all samples, corresponding to a yield less than

438   1.0% from parent compound photolysis.

3.4   Photoproducts of Chlorinated Phenoxyacetic Acid Herbicides on Surfaces

440   The 2,4,5-T and 2,4,5-TBEE surface samples were analyzed using HPLC and UPLC-

441   ESI(-)-qTOF. Figures 5C and 5D show the evolution of DBEEs and dichlorophenoxyacetic acids

442   from 2,4,5-TBEE and 2,4,5-T photolysis on surfaces, respectively, as determined by HPLC.

443   Concentrations of the dechlorination products of 2,4,5-TBEE (sum of 2,4-DBEE, 2,5-DBEE, and

444   3,4-DBEE) were quantified by HPLC as described in section 3.3. A similar method was also

445   used to quantify the concentrations of dechlorination products of 2,4,5-T, for which the sum of

446   2,4-D, 2,5-D, and 3,4-D was estimated using the HPLC calibration curve of 2,4-D.

19

447   In contrast to that observed in organic solvents, the amount of photoreductive

448   dechlorination products accounted for less than 60% of the parent compound decay on surfaces

449   on a molar basis. On wax surface, DBEEs accounted for 51–60% of 2,4,5-TBEE decay, while

450   dichlorophenoxyacetic acids accounted for 28–43% of 2,4,5-T decay; on quartz surface, the

451   percentage was even lower (10–42%). Similar to that observed in solvents, the yield of 2,4,5-

452   trichlorophenol from 2,4,5-T and 2,4,5-TBEE photolysis on surfaces was also less than 1.0%. A

453   recent study on the photoproducts of 2,4-D ethyl ester on glass surface and leaf cutin surface

454   proposed that 2,4-D ethyl ester can hydrolyze to form the corresponding acid (2,4-D),[60] but

455   2,4,5-T was not detected in the 2,4,5-TBEE surface samples, corresponding to a yield less than

456   1.5% from parent compound decay. These findings suggest that ester hydrolysis of 2,4,5-TBEE

457   did not appreciably occur in the examined systems.

458   For each surface experiment, additional samples were collected for UPLC-ESI(-)-qTOF

459   analysis at three time points: time zero (t_0), the time corresponding to ~25% parent compound

460   decay (t_m), and the time corresponding to approximately 90% parent compound decay or 48 h

461   whichever is shorter (t_f). Table 2 summarizes the results regarding the three groups of putative

462   photoproducts shown in Figure 4 for the t_f samples. None of these putative products were

463   detected in the t_0 or t_m samples with sufficient confidence. Dichlorophenoxyacetic acids were

464   detected from 2,4,5-T photolysis on surfaces, while DBEEs were not detected from 2,4,5-TBEE

465   photolysis. However, monochlorinated products were detected in both 2,4,5-T and 2,4,5-TBEE

466   samples, suggesting further decay of the dichlorinated products. The putative products

467   corresponding to photosubstitution of chlorine by a hydroxyl group (II) and the cleavage of the

468   ether bond (III) were not detected. The absence of DBEE signals in the UPLC-ESI(-)-qTOF

469   analysis for 2,4,5-TBEE is in contrast to their detection by HPLC (Figure 5C). It may be

470   attributed to the surfactant present in the extracts of surface samples, which can significantly

471   suppress ionization during the UPLC-ESI(-)-qTOF analyses. Overall, the UPLC-ESI(-)-qTOF

472   analysis of 2,4,5-T and 2,4,5-TBEE photoproducts confirmed the prevalence of the

473   photoreductive dechlorination pathway (I), but did not identify new products that can close the

474   mass balance for phenoxyacetic acid herbicide photolysis on surfaces. The analysis of 2,4-D and

475   2,4-DBEE photoproducts on quartz and wax surfaces by UPLC-ESI(-)-qTOF also did not yield

476   additional information (Table S6).

477   **3.5   Direct Photolysis Mechanism of Chlorinated Phenoxyacetic Acid Herbicides**

478   We observed that reductive dechlorination is the dominant pathway for the direct

479   photolysis of trichlorinated phenoxyacetic acid herbicides (2,4,5-TBEE and 2,4,5-TME) in

480   methanol, 2-propanol, and *n*-heptane (Figures 5A and 5B). Previously, the butyl, methyl, and

481   butoxyethyl esters of 2,4-D were also shown to undergo photoreductive dechlorination in hexane

482   and hexadecane.[43, 55] Our results suggest that photoreductive dechlorination can be important in

483   the more polar solvents methanol and 2-propanol. Additionally, the results also suggest that the

484   additional chlorine substitution on the aromatic ring does not significantly impact the reaction

485   pathways of chlorinated phenoxyacetic acid herbicides. The similar photolysis behavior between

486   the esters of 2,4,5-T and 2,4-D in organic solvents echoes the similarity in degradation pathways

487   between 2,4,5-T and 2,4-D in water.[43, 54, 59] Faster photolysis was observed in organic solvents of

488   lower polarity, where the quantum yields were higher (Figure 1 and 3). It was previously

489   proposed that polar solvents are more likely to interact with and to quench polarizable excited

490   states relative to less polar solvents; this rationale was used to explain the decrease in dioxin

491   direct photolysis rates with increasing solvent polarity.[8] This mechanism may also apply to our

492   systems.

493   Previous studies have investigated photolysis of 2,4-D and 2,4,5-T in water and reported

494   that the major pathways are photosubstitution of chlorine by a hydroxyl group and cleavage of

495   the ether bond (II and III in Figure 4), rather than reductive dechlorination.[54, 59] This difference in

496   pathways may account for the higher quantum yields of 2,4-D and 2,4,5-T in water than those in

497   methanol and acetonitrile, despite that water is a more polar solvent. Nevertheless, the quantum

498   yields of 2,4-D and 2,4,5-T in water is 3–9 times lower than those in 2-propanol.

499   In addition to polarity, H-donating ability also varies among acetonitrile, methanol, 2-

500   propanol, and *n*-heptane. Because the photoreductive dechlorination process involves the

501   generation of a radical via homolysis of the C-Cl bond in an excited molecule and subsequent

502   abstraction of a hydrogen atom from solvent,[9] the H-donating ability of solvent molecules may

503   also influence photolysis. Table S7 compares the dissociation energy of the weakest C-H bond in

504   the four solvent molecules.[61-64] *n*-Heptane has the highest C-H bond dissociation energy,

505   followed by methanol and acetonitrile, and then 2-propanol. Since the poorest H-donor (*n*-

506   heptane) exhibited the fastest photolysis, it can be concluded that H-abstraction is not rate-

507   limiting and that the H-donating ability of organic solvents does not appreciably influence

508   photolysis rate.

509   On quartz and paraffin wax surfaces, the chlorinated phenoxyacetic acid herbicides

510   degraded faster than or at comparable rates as in organic solvents of low polarity (Figure 1). The

511   fast photolysis on quartz was due to the high quantum yields rather than strong light absorption.

512   In fact, the light absorption of phenoxyacetic acid herbicides on quartz is lower than that in

513   organic solvents (Figure 2 and S2). Although the presence of surfactant in surface samples likely

514   hindered product analysis by UPLC-ESI(-)-qTOF, dechlorination was shown to be a prevalent

515   pathway for 2,4-D, 2,4,5-T, and their butoxyethyl esters. However, the apparent yields of the

516 dechlorination products (i.e., dichlorophenoxyacetic acids and DBEEs from 2,4,5-T and 2,4,5-

517 TBEE, respectively) on surfaces was much lower than those in organic solvents (Figure 5). There

518 are at least two possible reasons: (1) photoreductive dechlorination on surfaces is so facile that

519 the photoproducts rapidly undergo further dechlorination; and/or (2) alternative reaction

520 pathways are significant on surfaces. Assuming the first reason to be valid, a preliminary kinetic

521 model was developed for the accumulation of DBEEs from 2,4,5-TBEE photolysis on surfaces

522 (detailed description provided in Text S5). As shown in Figure S8, the time profile of DBEE

523 concentrations predicted by the model does not agree with the experimental results. This

524 suggests that the lower molar ratio of dechlorination products to parent compound decay on

525 surfaces should be attributed to alternative reaction pathways in parallel with reductive

526 dechlorination, and that these pathways are specific to surfaces. Further study is needed to

527 identify these pathways.

528 **4   Conclusion**

529   The direct photolysis of six chlorinated phenoxyacetic acid herbicides (2,4-D, 2,4,5-T

530 and their methyl and butoxyethyl esters) was investigated in organic solvents and on quartz and

531 paraffin wax surfaces under simulated sunlight. Photolysis was enhanced in solvents of low

532 polarity, and the enhancement was due to higher quantum yields rather than stronger light

533 absorption in these solvents. Photolysis on paraffin wax, a surface closely resembling leaf

534 cuticle,[9] was slower than that on quartz, but was comparable to that in organic solvents of low

535 polarity (i.e., *n*-heptane and 2-propanol). Under the environmentally-relevant conditions

536 employed in this study, most of the examined phenoxyacetic acid herbicides underwent

537 photolysis at rates on par with rates of biodegradation, the major dissipation pathway currently

538 considered for these herbicides.[52] These results suggest that photolysis on leaf surfaces can

539　appreciably influence the environmental fate of phenoxyacetic acid herbicides in the

540　environment.

541　　　Product analysis shows that photoreductive dechlorination is the dominant pathway in

542　organic solvents. While photoreductive dechlorination also plays an important role on quartz and

543　paraffin wax surfaces, it cannot account for all of the photodegradation as quantified by loss of

544　parent compounds. Photolysis on surface features unique pathways that requires further

545　investigation.

546

547　**Conflicts of interest**

548　　　The authors have no conflict of interest to declare.

549

550　**Acknowledgements**

553   Reference:

554   1.   T. Katagi, Photodegradation of pesticides on plant and soil surfaces, *Rev. Environ.*
555   *Contam. Toxicol.*, 2004, **182**, 1-189.
556   2.   C. K. Remucal, The role of indirect photochemical degradation in the environmental fate
557   of pesticides: a review, *Environ. Sci.: Processes Impacts*, 2014, **16**, 628-653.
558   3.   R. P. Schwarzenbach, P. M. Gschwend and D. M. Imboden, *Environmental organic*
559   *chemistry*, Wiley, Hoboken, N.J., 2nd edn., 2003.
560   4.   T. Zeng and W. A. Arnold, Pesticide photolysis in prairie potholes: probing
561   photosensitized processes, *Environ. Sci. Technol.*, 2012, **47**, 6735-6745.
562   5.   M. W. Lam, K. Tantuco and S. A. Mabury, PhotoFate: A new approach in accounting for
563   the contribution of indirect photolysis of pesticides and pharmaceuticals in surface
564   waters, *Environ. Sci. Technol.*, 2003, **37**, 899-907.
565   6.   B. Eyheraguibel, A. ter Halle and C. Richard, Photodegradation of bentazon, clopyralid,
566   and triclopyr on model leaves: Importance of a systematic evaluation of pesticide
567   photostability on crops, *J. Agric. Food Chem.*, 2009, **57**, 1960-1966.
568   7.   K. Koch, B. Bhushan and W. Barthlott, Multifunctional surface structures of plants: An
569   inspiration for biomimetics, *Prog. Mater. Sci.*, 2009, **54**, 137-178.
570   8.   J. Choi, W. Choi and B. J. Mhin, Solvent-specific photolytic behavior of
571   octachlorodibenzo-p-dioxin, *Environ. Sci. Technol.*, 2004, **38**, 2082-2088.
572   9.   J. Dolinova, A. Klanova, P. Klan and I. Holoubek, Photodegradation of organic
573   pollutants on the spruce needle wax surface under laboratory conditions, *Chemosphere*,
574   2004, **57**, 1399-1407.
575   10.   V. Ramamurthy, Organic photochemistry in organized media, *Tetrahedron*, 1986, **42**,
576   5753-5839.
577   11.   W. Schwack and H. Flößer-Müller, Fungicides and photochemistry. Photodehalogenation
578   of captan, *Chemosphere*, 1990, **21**, 905-912.
579   12.   W. Schwack, W. Andlauer and W. Armbruster, Photochemistry of parathion in the plant
580   cuticle environment: Model reactions in the presence of 2-propanol and methyl 12-
581   hydroxystearate, *Pest Manag. Sci.*, 1994, **40**, 279-284.
582   13.   W. Schwack, Photoinduced additions of pesticides to biomolecules. 2. Model reactions of
583   DDT and methoxychlor with methyl oleate, *J. Agric. Food Chem.*, 1988, **36**, 645-648.
584   14.   D. E. Breithaupt and W. Schwack, Photoinduced addition of the fungicide anilazine to
585   cyclohexene and methyl oleate as model compounds of plant cuticle constituents,
586   *Chemosphere*, 2000, **41**, 1401-1406.
587   15.   P. Sandin-Espana, B. Sevilla-Moran, C. Lopez-Goti, M. M. Mateo-Miranda and J. L.
588   Alonso-Prados, Rapid photodegradation of clethodim and sethoxydim herbicides in soil
589   and plant surface model systems, *Arabian J. Chem.*, 2016, **9**, 694-703.
590   16.   Z. Chen, M. J. Zabik and R. A. Leavitt, Comparative study of thin film photodegradative
591   rates for 36 pesticides, *Ind. Eng. Chem. Prod. Res. Dev.*, 1984, **23**, 5-11.
592   17.   D. G. Crosby and A. S. Wong, Environmental degradation of 2, 3, 7, 8-
593   tetrachlorodibenzo-p-dioxin (TCDD), *Science*, 1977, **195**, 1337-1338.
594   18.   K. Sato, Y. Kato, S. Maki, O. Matano and S. Goto, Photolysis of fungicide guazatine on
595   glass surfaces, *J. Pestic. Sci.*, 1985.
596   19.   N. Schippers and W. Schwack, Photochemistry of imidacloprid in model systems, *J.*
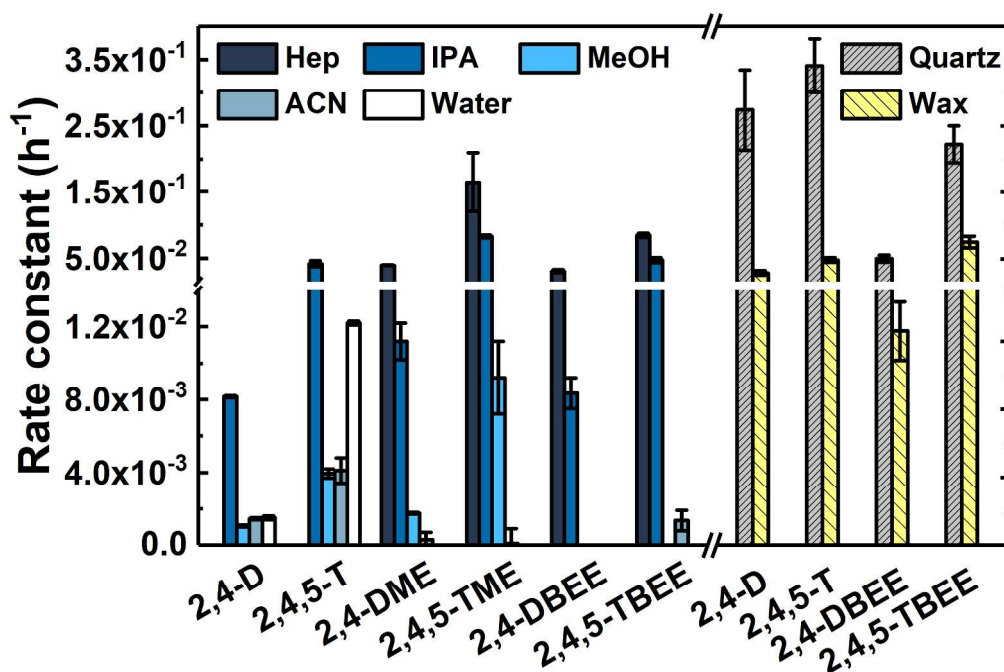597   *Agric. Food Chem.*, 2008, **56**, 8023-8029.

598   20.   M. Fukushima and T. Katagi, Photodegradation of fenitrothion and parathion in tomato
599   epicuticular waxes, *J. Agric. Food Chem.*, 2006, **54**, 474-479.
600   21.   J. P. Da Silva, L. F. Vieira Ferreira, A. M. Da Silva and A. S. Oliveira, Photochemistry of
601   4-chlorophenol on cellulose and silica, *Environ. Sci. Technol.*, 2003, **37**, 4798-4803.
602   22.   P. Cabras, A. Angioni, V. L. Garau, M. Melis, F. M. Pirisi and E. V. Minelli, Effect of
603   epicuticular waxes of fruits on the photodegradation of fenthion, *J. Agric. Food Chem.*,
604   1997, **45**, 3681-3683.
605   23.   F. Schuler, P. Schmid and C. H. Schlatter, Photodegradation of polychlorinated dibenzo-
606   p-dioxins and dibenzofurans in cuticular waxes of laurel cherry (Prunus laurocerasus),
607   *Chemosphere*, 1998, **36**, 21-34.
608   24.   R. Riccio, M. Trevisan and E. Capri, Effect of surface waxes on the persistence of
609   chlorpyrifos-methyl in apples, strawberries and grapefruits, *Food Addit. Contam.*, 2006,
610   **23**, 683-692.
611   25.   F. Schynowski and W. Schwack, Photochemistry of parathion on plant surfaces:
612   relationship between photodecomposition and iodine number of the plant cuticle,
613   *Chemosphere*, 1996, **33**, 2255-2262.
614   26.   A. Ter Halle, D. Drncova and C. Richard, Phototransformation of the herbicide
615   sulcotrione on maize cuticular wax, *Environ. Sci. Technol.*, 2006, **40**, 2989-2995.
616   27.   J. R. Plimmer and U. I. Klingebiel, Photolysis of hexachlorobenzene, *J. Agric. Food
617   Chem.*, 1976, **24**, 721-723.
618   28.   D. Lavieille, A. ter Halle and C. Richard, Understanding mesotrione photochemistry
619   when applied on leaves, *Environ. Chem.*, 2008, **5**, 420-425.
620   29.   Z. Zhou, Y. Yang, Z. Zheng and M. Wang, Photodegradation of the benzothiostrobin in
621   solution and on soil and glass surface, *Water Sci. Technol.*, 2017, **76**, 364-372.
622   30.   D. Lavieille, A. Ter Halle, P.-O. Bussiere and C. Richard, Effect of a spreading adjuvant
623   on mesotrione photolysis on wax films, *J. Agric. Food Chem.*, 2009, **57**, 9624-9628.
624   31.   A. Grube, D. Donaldson, T. Kiely and L. Wu, Pesticides industry sales and usage, *US
625   EPA, Washington, DC*, 2011.
626   32.   D. Edwards, Reregistration Eligibility Decision for 2,4-D,
627   https://archive.epa.gov/pesticides/reregistration/web/pdf/24d_red.pdf, (accessed April 04,
628   2018).
629   33.   D. McMartin, J. Gillies, J. Headley and H. Peterson, Biodegradation kinetics of 2, 4-
630   dichlorophenoxyacetic acid (2, 4-D) in south saskatchewan river water, *Can. Water
631   Resour. J.*, 2000, **25**, 81-92.
632   34.   Q. Hee, Phenoxyalkanoic herbicides: Volume I, Chemistry, Analysis and environmental
633   pollution, *CRC PRESS, INC., BOCA RATON, FL. 1981.*, 1981.
634   35.   Decision Guidance Documents 2,4,5-T and its salts and esters
635   http://www.pic.int/Portals/5/DGDs/DGD_2,4,5-T_EN.pdf, (accessed June 11, 2018).
636   36.   I. Southern Agricultural Ins. and F. Palmetto, 2,4-D Amine Weed Killer Selective
637   Broadleaf Weed Control, http://www.rrsi.com/wp-content/uploads/2014/05/24-
638   D_Amine_Weed_Killer_LABEL1.pdf, (accessed July 01, 2017).
639   37.   R. G. Zepp, Quantum yields for reaction of pollutants in dilute aqueous solution, *Environ.
640   Sci. Technol.*, 1978, **12**, 327-329.
641   38.   E. S. Galbavy, K. Ram and C. Anastasio, 2-Nitrobenzaldehyde as a chemical actinometer
642   for solution and ice photochemistry, *J. Photochem. Photobiol., A*, 2010, **209**, 186-192.

643 39. G. J. Phillips and W. R. Simpson, Verification of snowpack radiation transfer models
644   using actinometry, *J. Geophys. Res.*, 2005, **110**, 8.
645 40. P. A. Leighton and F. A. Lucy, Photoisomerization of the o-nitrobenzaldehydes. II.
646   Mathematical treatment, *J. Chem. Phys.*, 1934, **2**, 760-766.
647 41. J. C. S. M. V. George, Photochemistry of o-nitrobenzaldehyde and related studies, *J.
648   Phys. Chem.*, 1980, **84**, 492–495.
649 42. J. M. Allen, S. K. Allen and S. W. Baertschi, 2-Nitrobenzaldehyde: a convenient UV-A
650   and UV-B chemical actinometer for drug photostability testing, *J. Pharm. Biomed. Anal.*,
651   2000, **24**, 167-178.
652 43. R. G. Zepp, N. L. Wolfe, J. A. Gordon and G. L. Baughman, Dynamics of 2,4-D esters in
653   surface waters. Hydrolysis, photolysis, and vaporization, *Environ. Sci. Technol.*, 1975, **9**,
654   1144-1150.
655 44. L.-S. Hung and L. L. Ingram, Effect of solvents on the photodegradation rates of
656   octachlorodibenzo-p-dioxin, *Bull. Environ. Conam. Toxicol.*, 1990, **44**, 380-386.
657 45. J. Chastain, A. Ter Halle, P. de Sainte Claire, G. Voyard, M. Traikïa and C. Richard,
658   Phototransformation of azoxystrobin fungicide in organic solvents. Photoisomerization
659   vs. photodegradation, *Photochem. Photobiol. Sci.*, 2013, **12**, 2076-2083.
660 46. V. Librando, G. Bracchitta, G. de Guidi, Z. Minniti, G. Perrini and A. Catalfo,
661   Photodegradation of anthracene and benzo [a] anthracene in polar and apolar media: new
662   pathways of photodegradation, *Polycyclic Aromat. Compd.*, 2014, **34**, 263-279.
663 47. S.-P. Wu, J. Schwab, B.-Y. Yang and C.-S. Yuan, Effect of phenolic compounds on
664   photodegradation of anthracene and benzo [a] anthracene in media of different polarity, *J.
665   Photochem. Photobiol., A*, 2015, **309**, 55-64.
666 48. I. Ahmad, Z. Anwar, S. Ahmed, M. A. Sheraz, R. Bano and A. Hafeez, Solvent effect on
667   the photolysis of riboflavin, *AAPS PharmSciTech*, 2015, **16**, 1122-1128.
668 49. P. P. Choudhury, Leaf cuticle-assisted phototransformation of isoproturon, *Acta Physiol.
669   Plant.*, 2017, **39**, 188.
670 50. M. Sleiman, P. de Sainte Claire and C. Richard, Heterogeneous photochemistry of
671   agrochemicals at the leaf surface: a case study of plant activator acibenzolar-S-methyl, *J.
672   Agric. Food Chem.*, 2017, **65**, 7653-7660.
673 51. M. B. McConville, N. M. Cohen, S. M. Nowicki, S. R. Lantz, J. L. Hixson, A. S. Ward
674   and C. K. Remucal, A field analysis of lampricide photodegradation in Great Lakes
675   tributaries, *Environ. Sci.: Processes Impacts*, 2017, **19**, 891-900.
676 52. O. M. Aly and S. D. Faust, Herbicides in surface waters, studies on fate of 2, 4-D and
677   ester derivatives in natural surface waters, *J. Agric. Food Chem.*, 1964, **12**, 541-546.
678 53. K. Z. Aregahegn, D. Shemesh, R. B. Gerber and B. J. Finlayson-Pitts, Photochemistry of
679   thin solid films of the neonicotinoid imidacloprid on surfaces, *Environ. Sci. Technol.*,
680   2017, **51**, 2660-2668.
681 54. D. G. Crosby and H. O. Tutass, Photodecomposition of 2, 4-dichlorophenoxyacetic acid,
682   *J. Agric. Food Chem.*, 1966, **14**, 596-599.
683 55. S. S. Q. Hee, S. H. Paine and R. G. Sutherland, Photodecomposition of a formulated
684   mixed butyl ester of 2, 4-dichlorophenoxyacetic acid in aqueous and hexane solutions, *J.
685   Agric. Food Chem.*, 1979, **27**, 79-82.
686 56. CSID:31290797, http://www.chemspider.com/Chemical-Structure.31290797.html,
687   (accessed April 05, 2018).

688   57.   CSID:1443, http://www.chemspider.com/Chemical-Structure.1443.html, (accessed April
689   05, 2018).
690   58.   CSID:26055484, http://www.chemspider.com/Chemical-Structure.26055484.html,
691   (accessed April 05, 2018).
692   59.   D. G. Crosby and A. S. Wong, Photodecomposition of 2, 4, 5-trichlorophenoxyacetic
693   acid (2, 4, 5-T) in water, *J. Agric. Food Chem.*, 1973, **21**, 1052-1054.
694   60.   P. P. Choudhury, Leaf-cutin assisted phototransformation of 2, 4-D ethyl ester, *Indian J.*
695   *Biochem. Biophys.*, 2016, **53**, 227-231.
696   61.   Q. Xie, J. Chen, J. Shao, H. Zhao and C. Hao, Important role of reaction field in
697   photodegradation of deca-bromodiphenyl ether: theoretical and experimental
698   investigations of solvent effects, *Chemosphere*, 2009, **76**, 1486-1490.
699   62.   D. E. Lewis, *Advanced organic chemistry*, Oxford University Press, 2016.
700   63.   Y.-R. Luo, *Comprehensive handbook of chemical bond energies*, CRC press, 2007.
701   64.   X. Zeng, R. Qu, M. Feng, J. Chen, L. Wang and Z. Wang, Photodegradation of
702   polyfluorinated dibenzo-p-dioxins in organic solvents: experimental and theoretical
703   studiesd, *Environ. Sci. Technol.*, 2016, **50**, 8128-8134.
704

1
2
3
4
5
6
7
8
9
10
11
12
13
14
15
16
17
18
19

705 **Figures:**
706 Figure 1. Apparent first-order photolysis rate constants for 2,4-D, 2,4,5-T, and their methyl and
707 butoxyethyl esters in different solvents (open and blue shaded bars), and on quartz and paraffin
708 wax surfaces (hatched bars). Error bars represent the standard deviation of duplicate
709 experiments. Hep = n-heptane, IPA = 2-propanol, MeOH = methanol, ACN = acetonitrile,
710 Quartz = quartz surface, Wax = paraffin wax surface. The values of the apparent first-order
711 photolysis rate constants are listed in Table S3. Conditions: the sunlight simulator intensity was
712 set to 0.68 W m^{-2} at 340 nm, with total irradiation of 320 W m^{-2} as determined by the
713 actinometer 2-NB; initial concentration: 20 µM for 2,4-D and 2,4,5-T, and 5 µM for esters; 5
714 mM phosphate buffer (pH 7.0) for experiments in water; 26 °C. Initial surface pesticide
715 concentration: 3×10^{-9} mol cm^{-2} on quartz or paraffin wax surface; surfactant (Tween$^{®}$ 20)
716 concentration: 3×10^{-9} mol cm^{-2} on quartz surface, and 3×10^{-8} mol cm^{-2} on paraffin wax
717 surface. 2,4-D and 2,4,5-T were not evaluated in n-heptane; esters were not evaluated in water;
718 2,4-DBEE and 2,4,5-TBEE were not evaluated in methanol.

20
21
22
23
24
25
26
27
28
29
30
31
32
33
34
35
36
37
38
39
40

719

41
42
43
44
45
46
47
48
49
50
51
52
53
54
55
56
57
58
59
60

720 Figure 2. Molar extinction coefficients of 2,4-D in solvents and on quartz surface. IPA = 2-
721 propanol, MeOH = methanol, ACN = acetonitrile, Quartz = quartz surface. Absorbance was
722 measured using a 20 μM aqueous sample (5 mM phosphate buffer, pH 7.0), a 5 μM organic
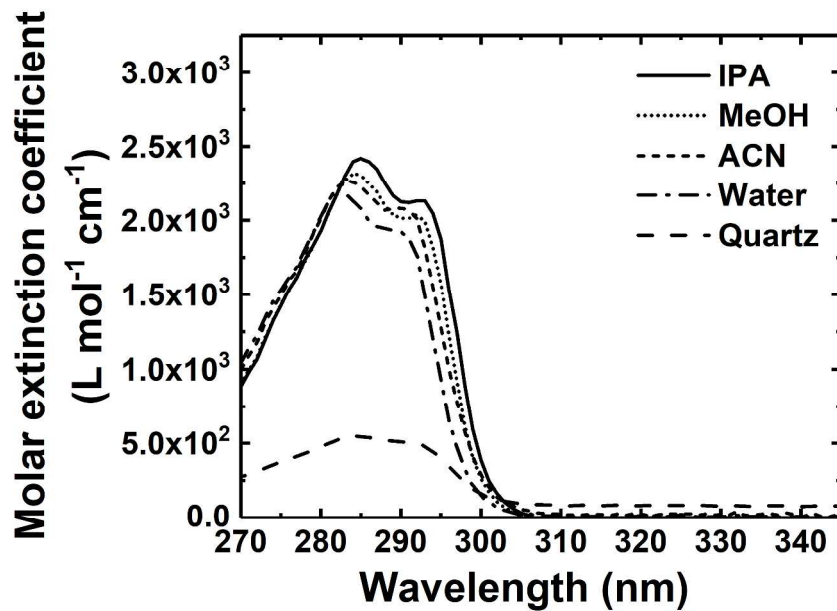723 solvent samples, and a 6.17×10^{-8} mol cm^{-2} quartz surface sample, respectively.

724

725   Figure 3. Quantum yields for the direct photolysis of 2,4-D, 2,4,5-T, and their esters in different
726   solvents. Error bars represent the standard deviation of duplicate experiments. Hep = *n*-heptane,
727   IPA = 2-propanol, MeOH = methanol, ACN = acetonitrile. The values of the quantum yields are
728   listed in Table S3. 2,4-D and 2,4,5-T were not evaluated in *n*-heptane; esters were not evaluated
729   in water; 2,4-DBEE and 2,4,5-TBEE were not evaluated in methanol.

730
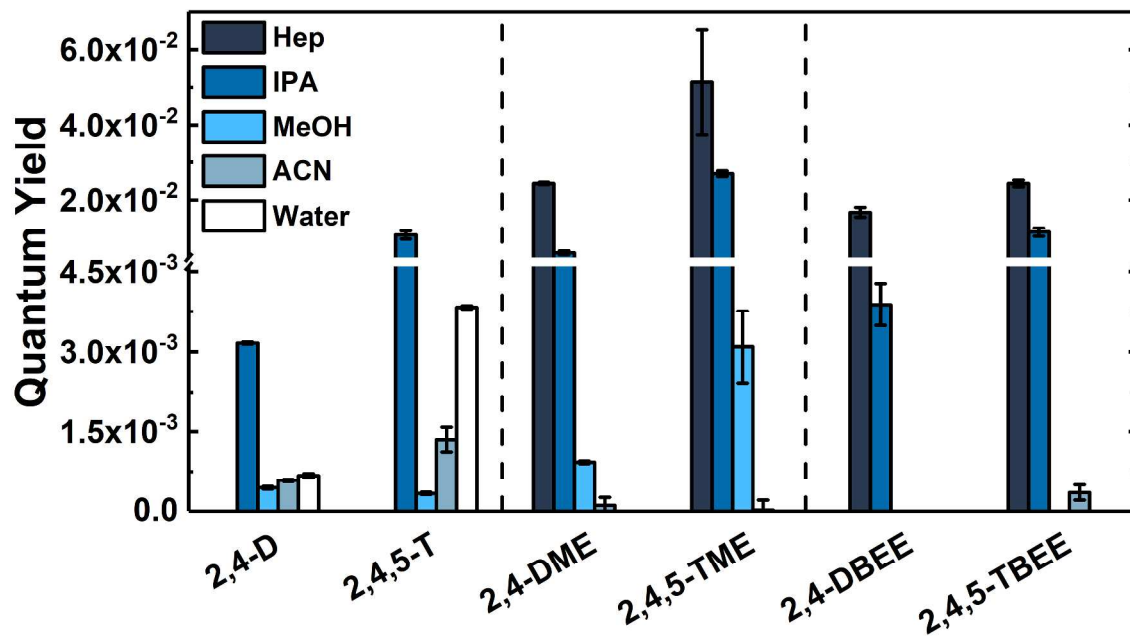
731

732 Figure 4. Putative photolysis pathways of chlorinated phenoxyacetic acid herbicides: (I)
733 photoreductive dechlorination, (II) photosubstitution of chlorine by a hydroxyl group, and (III)
734 cleavage of the ether bond.
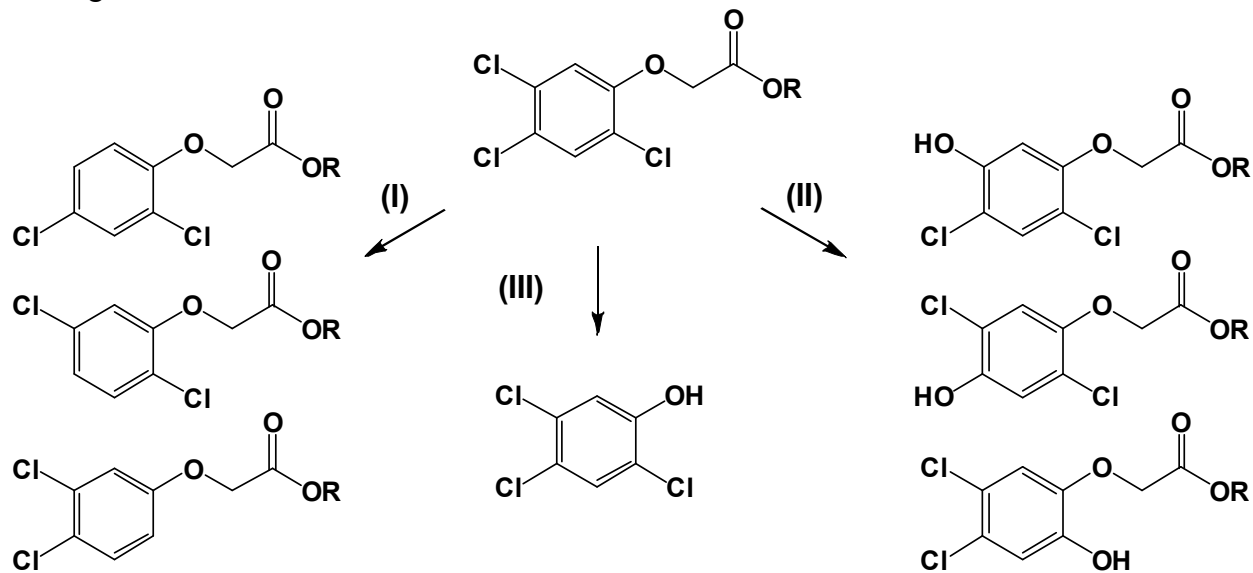
735 R = H, CH₃, (CH₂)₂O(CH₂)₃CH₃

736   Figure 5. Formation of reductive dechlorination products from the photolysis of (A) 2,4,5-TBEE
737   and (B) 2,4,5-TME in organic solvents, and (C) 2,4,5-TBEE and (D) 2,4,5-T on surfaces. Hep =
738   *n*-heptane, IPA = 2-propanol, MeOH = methanol, Quartz = quartz surface, Wax = paraffin wax
739   surface. Conditions: the sunlight simulator intensity was set to 0.68 W m^{-2} at 340 nm; initial
740   concentration of parent compound: 10 µM in organic solvents and 3×10^{-9} mol cm^{-2} on surfaces;
741   26 °C. DBEEs = $\sum$ (2,4-DBEE, 2,5-DBEE, 3,4-DBEE), DMEs = $\sum$ (2,4-DME, 2,5-DME, 3,4-
742   DME), and Ds = $\sum$ (2,4-D, 2,5-D, 3,4-D). Dash lines correspond to 1:1 stoichiometric
743   conversion from the parent compound to the product.
744   (A)
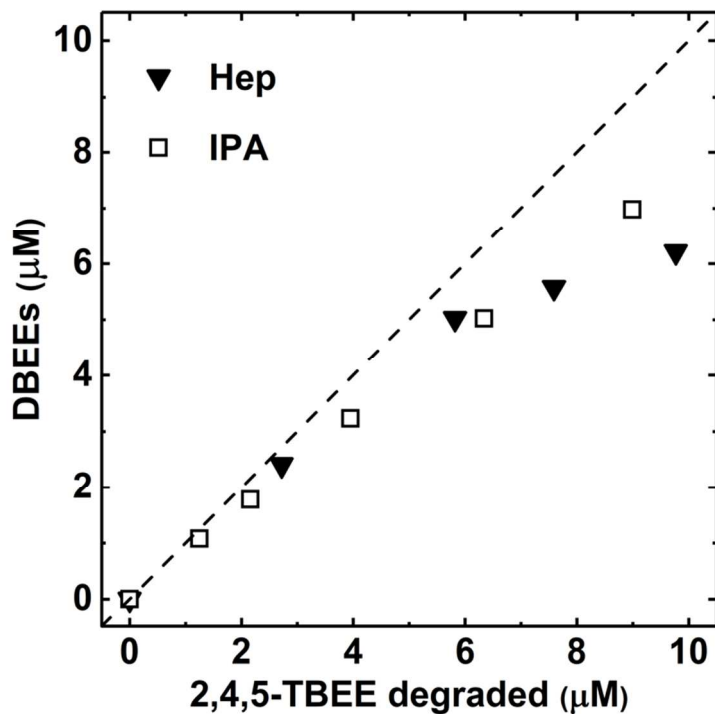
745

746   (B)
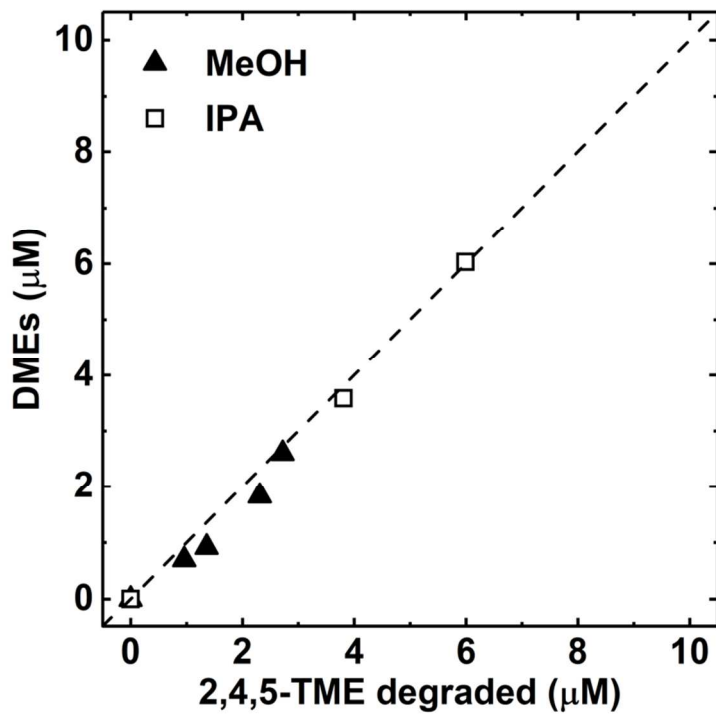
747
748   (C)
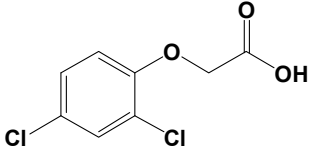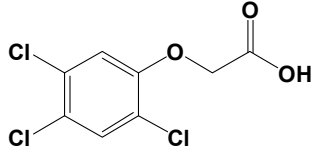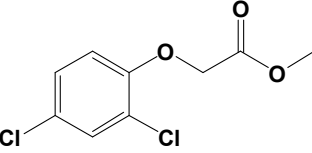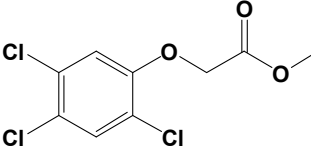

749

750   (D)
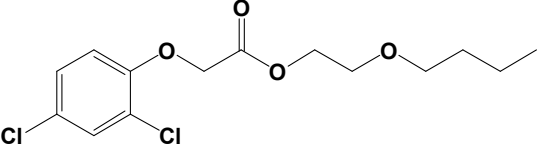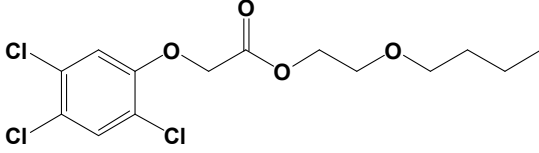

751
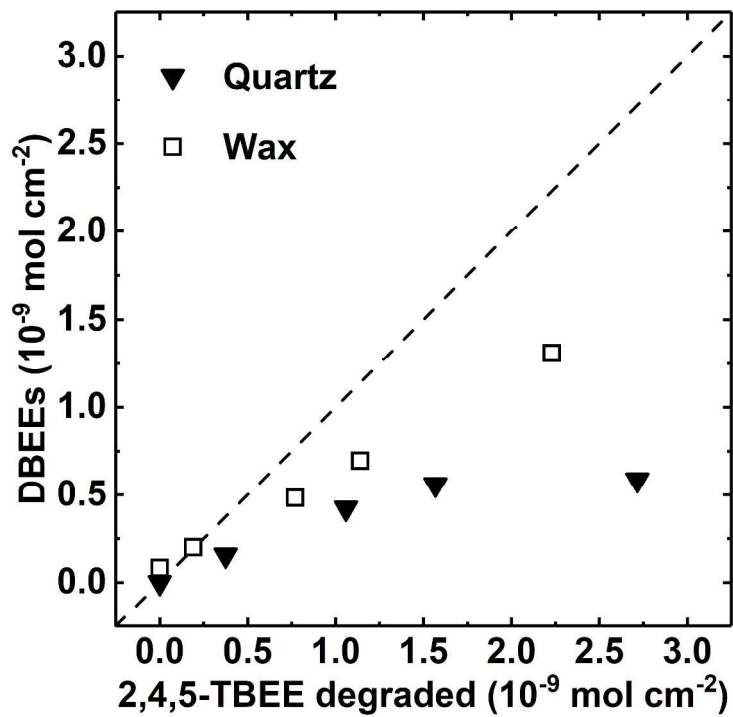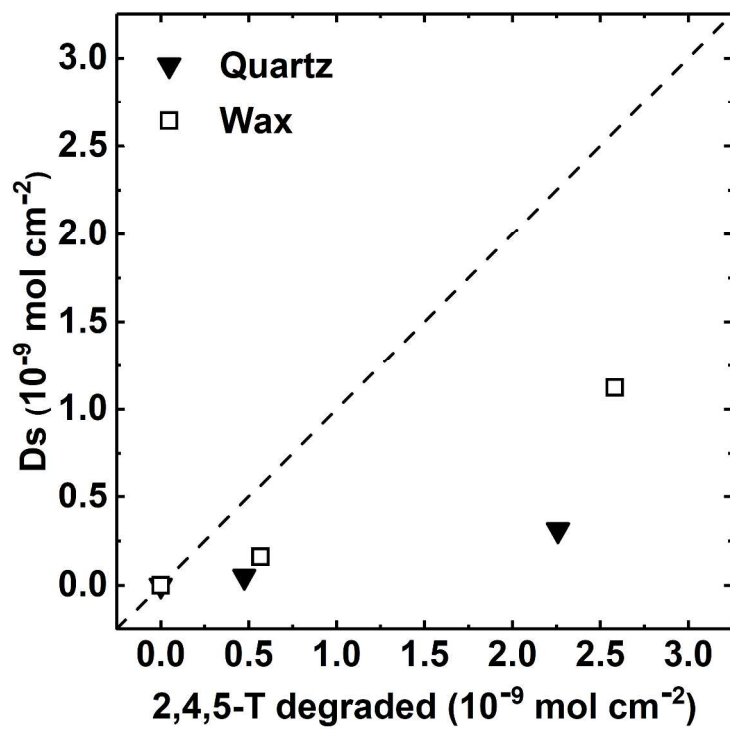
752   Figure 6. Gas chromatogram for 2,4,5-TME and its degradation products after 12 h irradiation in
753   *n*-heptane. GC-MS conditions: Initial column temperature was set at 90°C and held for 1 min,
754   and then increased to 270 °C at a rate of 100 °C min^{-1} and held for 10 min. MS full scan with
755   chemical ionization using methanol. The mass range of the MS scan was 50–400 m/z.

756
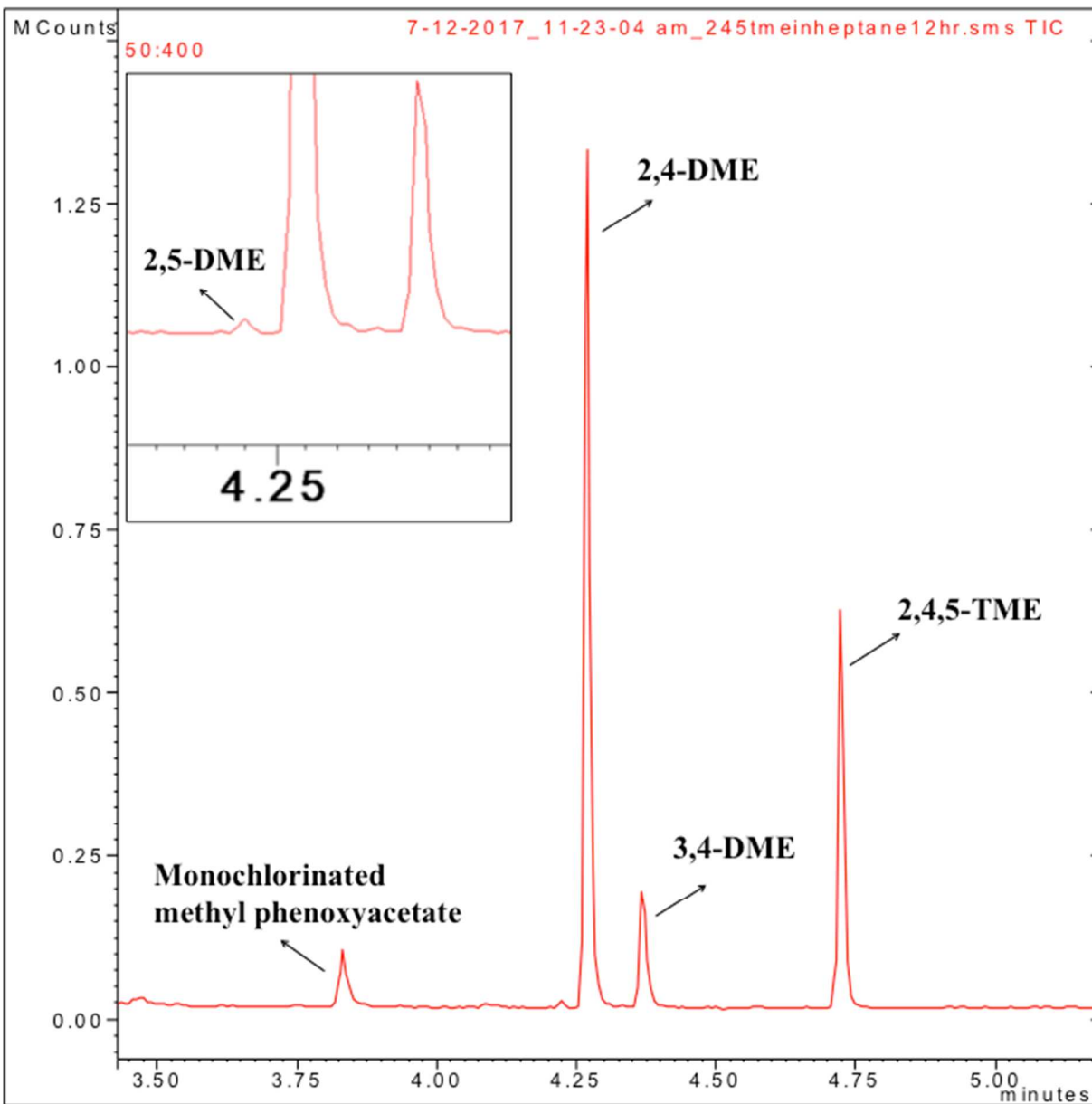
757 Table 1. Chemical structure of the six chlorinated phenoxyacetic acid herbicides investigated in
758 this study.

2,4-dichlorophenoxyacetic acid (2,4-D)	2,4,5-trichlorophenoxyacetic acid (2,4,5-T)
2,4-D methyl ester (2,4-DME)	2,4,5-T methyl ester (2,4,5-TME)
2,4-D butoxyethyl ester (2,4-DBEE)	2,4,5-T butoxyethyl ester (2,4,5-TBEE)

759

760 Table 2. Photoproducts of 2,4,5-T and 2,4,5-TBEE analyzed by UPLC-ESI(-)-qTOF.[a] The three
761 groups of putative photoproducts (I), (II), and (III) correspond to the structures in Figure 4. t_f =
762 reaction time corresponding to approximately 90% parent compound decay or 48 h, whichever is
763 shorter; RT = retention time; m/z = measured mass-to-charge ratio; Δ m/z = (measured m/z –
764 calculated m/z) / calculated m/z × 10^6; N.D. = not detected.

Parent compound	Surface	t_f (h)	Parent decay	Putative products (I)[b]		(II)[c]	(III)[d]
				Dichlorinated	Monochlorinated		
2,4,5-T	Quartz	6	87%	Detected[e] RT = 3.73 min m/z = 218.9620 Δ m/z = 1.8 ppm	Detected[e] RT = 1.62 min m/z = 185.0004 Δ m/z = –0.5 ppm	N.D.	N.D.
	Wax	48	90%	Detected[e] RT = 3.69 min m/z = 218.9624 Δ m/z = 3.7 ppm	Detected (weak signal)[e] RT = 1.62 min m/z = 185.0020 Δ m/z = 8.1 ppm	N.D.	N.D.
2,4,5-TBEE	Quartz	6	73%	N.D	Detected[e] RT = 7.74 min m/z = 285.0834 Δ m/z = –21 ppm	N.D.	N.D.
	Wax	48	98%	N.D	Detected[e] RT = 7.71 min m/z = 285.0899 Δ m/z = 1.8 ppm	N.D.	N.D.

765 [a] Product identification was based on measurements of exact masses; authentic standards were
766 not used.
767 [b] Reductive dechlorination products: dichlorinated and monochlorianted phenoxyacetic acids or
768 butoxyethyl phenoxyacetates, corresponding to pathway (I) in Figure 4.
769 [c] Products formed through photosubstitution of chlorine by a hydroxyl group, corresponding to
770 pathway (II) in Figure 4.
771 [d] Ether bond cleavage product 2,4,5-trichlorophenol, corresponding to pathway (III) in Figure 4.
772 [e] It is unknown which isomer(s) is/are represented by this peak.

1

1
2
3
4
5
6
7
8
9
10
11
12
13
14
15
16
17
18
19
20
21
22
23
24
25
26
27
28
29
30
31
32
33
34
35
36
37
38
39
40
41
42
43
44
45
46
47
48
49
50
51
52
53
54
55
56
57
58
59
60

$t_{1/2}$ Photo,surface $\approx t_{1/2}$ Bio

Φsurface > Φwater

Unknown Products